

# Material Design and Qualification on Power InGaP HBTs for 2.4 GHz Transmitter Application

JianJang Huang, M. Hattendorf, Milton Feng

Center for Compound Semiconductor Microelectronics  
Department of Electrical and Computer Engineering  
The University of Illinois at Urbana-Champaign  
208 North Wright Street, Urbana, IL 61801 USA  
[jhuang6@students.uiuc.edu](mailto:jhuang6@students.uiuc.edu)  
Fax: (217)244-3662

Quesnell Hartmann and David Ahmari

Epiworks, Inc.  
1606 Rion Drive Champaign, IL 61822

## Abstract

To meet the requirement for today's 2.4GHz high power circuit applications, we designed and processed high power heterojunction bipolar transistors (HBTs). The InGaP/GaAs HBTs with current gain 52.2,  $BV_{CEO}=16.1V$ ,  $BV_{BCO}=24.6V$ ,  $f_t=39GHz$  and  $f_{max}=139GHz$  were achieved from a  $3 \times 10 \mu m^2$  emitter contact. The performance meets the specifications required.

## Introduction

The InGaP/GaAs HBT has become an excellent candidate for high power, high frequency applications due to its superior performance and reliability. To meet the requirement for today's 2.4GHz high power circuit applications, we designed and processed high power HBTs with high uniformity and manufacturability. The specifications of the power devices are, current gain  $\beta > 50$ , emitter-collector breakdown voltage  $BV_{CEO} > 14V$ , base-collector breakdown voltage  $BV_{BCO} > 20V$ ,  $f_t > 30GHz$  and  $f_{max} > 50GHz$ . Based on the theoretical predictions [1] and previous published works [2], three layer structures were proposed. The samples were then grown by MOCVD and processed on the 3-inch GaAs wafers. The current gain and breakdown voltage are compared in the small and large emitter area devices. Finally, high frequency response  $f_t$  and  $f_{max}$  are discussed.

To fabricate high power, i.e., high breakdown voltage (especially  $BV_{ceo}$  and  $BV_{bco}$ ) devices, a tradeoff is made in  $f_t$  vs  $BV_{CEO}$  (and  $BV_{BCO}$ ), since high speed and high power applications require different layer structures. A thinner collector is required for high speed devices, while a thicker collector and lower doping are desired for high power applications. In this work, to increase the breakdown voltage,  $BV_{CEO}$ , from 5V [2] to 14V, we doubled the thickness of the collector layer from the high frequency layer design [2, 3].  $F_t$

is therefore decreased but still far above the current demand of 2.4GHz blue tooth wireless circuit applications.

## Layer Structures

The layer structures are shown in Table 1. We compared the performance of three wafers with various collector designs. Sample A and B employed a collector thickness 800nm with doping  $10^{16} cm^{-3}$  and  $3 \times 10^{16} cm^{-3}$ , respectively. Sample C has a thicker collector, 900nm, and a collector doping density,  $10^{16} cm^{-3}$ .

## Device Processing

The InGaP/GaAs HBT process begins with a deposition of emitter contact (TiPtAu), which is also used to mask the emitter etch. The InGaAs contact layer and GaAs emitter cap were etched in a citric acid-based etch, while InGaP emitter was selectively etched in an HCl-based etch. The TiPtAu base metal was deposited and base and collector layers were etched. After the isolation etching, AuGeNiAu collector metal were deposited and alloyed. Polyimide planarization was followed and then a TiAu metallization was coated for cascade probing. Finally, Au air-bridge was evaporated to connect emitter and ground plane.

## DC performance for devices with emitter size $60 \times 60 \mu m^2$

A typical gummel plot is shown in Fig. 1, with base and collector ideality factor for sample C 1.06 and 1.0, respectively. The common emitter current gain at  $I_c=1mA$  is 117.6. Table 2 summarizes the DC results for sample A, B and C. The  $BV_{CEO}$  in each sample is larger than 16V and  $BV_{BCO}$  is larger than 22V due to their thicker collector layers. The typical  $I_c-V_{ce}$  curves for sample C are shown in Fig. 2 with  $I_b$  ranging from 0 to  $180 \mu A$  and  $V_{ce}=0$  to 10V. Those

Layer Designation	Material	Sample A	Sample B	Sample C
Emitter Cap	InGaAs (50%)	30nm, Si=2e19	30nm, Si=2e19	30nm, Si=2e19
Emitter Cap	InGaAs(Grade)	30nm, Si>1e19	30nm, Si>1e19	30nm, Si>1e19
Emitter Cap	GaAs	100nm, Si=4e18	100nm, Si=4e18	100nm, Si=4e18
Emitter	InGaP(In(0.49))	30nm, Si=3e17	30nm, Si=3e17	30nm, Si=3e17
Base	GaAs	140nm, C=2e19	140nm, C=2e19	140nm, C=2e19
Collector	GaAs	800nm, Si=1e16	800nm, Si=3e16	900nm, Si=1e16
Etch-stop	InGaP (50%)	20nm, Si=5e18	20nm, Si=5e18	20nm, Si=5e18
Subcollector	GaAs	500nm, Si=5e18	500nm, Si=5e18	500nm, Si=5e18
Substrate	GaAs	S.I.	S.I.	S.I.

Table 1. Layer structures for sample A, B and C

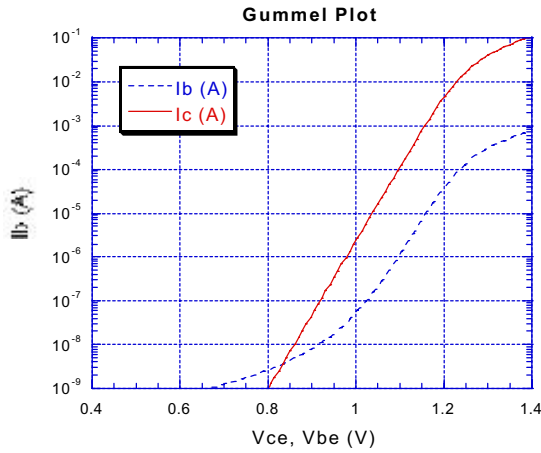


Fig. 1 Gummel plot for Sample C with a 60x60 $\mu\text{m}^2$  emitter contact

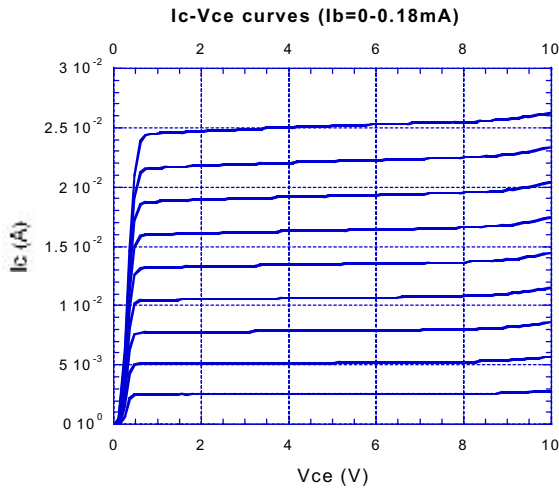


Fig. 2 Common emitter  $I_c$ - $V_{ce}$  characteristic for Sample C with the base current from 0 to 180 $\mu\text{A}$  in 20 $\mu\text{A}$  steps. The emitter size is 60x60 $\mu\text{m}^2$

DC parameters are in excellent uniformity across the 3 inch wafers.

#### DC performance for devices with emitter size 3x10 $\mu\text{m}^2$

In Fig. 3, the decrease of current gain was observed in devices with smaller Area/Perimeter (A/P) ratio due to the base layer surface recombination. The current gain of sample C is reduced from 117.6 of emitter size 60x60 $\mu\text{m}^2$  to 51.8 of 3x10 $\mu\text{m}^2$  under the same collector current,  $I_c=1\text{mA}$ . A passivated ledge structure can be a good resolution to avoid the decrease in current gain. Within a 1 $\mu\text{m}$  emitter-base spacing (the emitter layer undercut is around 0.2 $\mu\text{m}$ ), the surface recombination current doesn't change too much. However, we saw a decrease in current gain when the Emitter-Base spacing is above 2 $\mu\text{m}$ .

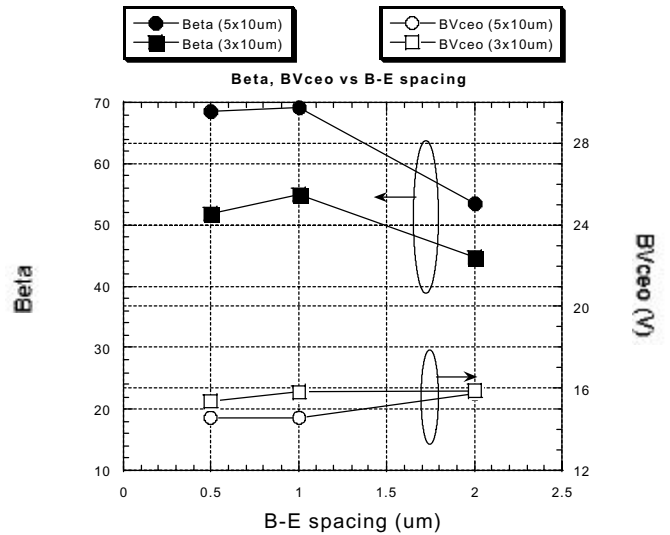


Fig. 3 Beta and  $BV_{CEO}$  vs Base-Emitter spacing of sample C.

Sample	Avg	$n_b$	$n_c$	$V_{th}$ 1 $\mu A$	$\beta_{@10}$ $\mu A$	$\beta_{@1}$ mA	$\beta_{max}$	$V_{off}$ (mV)	$BV_{cb}$ (V)	$BV_{ce}$ (V)	$BV_{eb}$ (V)	Res (/sq)	Rbs (/sq)
	Std												
A	$\mu$	1.032	1	0.982	70.7	82.2	97.9	180	24.6	16.4	6	71.3	216.4
	$\sigma^2$	0.004	0	0.002	2.02	2.85	3.32	0	0.89	1.48	0	1.09	1.817
B	$\mu$	1.054	1	0.982	67.9	81.26	88.8	180	22.5	19.8	6.16	96.88	293.2
	$\sigma^2$	0.009	0	0	3.25	2.688	3.1	0	0	1.57	0.09	1.13	5.119
C	$\mu$	1.058	1	0.977	87.0	117.6	150	180	26.8	16.4	5.54	106.9	306.8
	$\sigma^2$	0.004	0	0.001	1.92	5.27	5.79	0	0.45	1.54	0	13.8	9.783

Table 2. DC performance of sample A, B and C.

Sample	$BV_{CEO}$ (V)	Beta	$f_t$ (GHz)	$f_{max}$ (GHz)
A	15.5	37.1	38.0	132.0
B	18.2	38.0	38.9	135.0
C	16.1	52.2	39.1	139.0

Table 3. DC and RF performance of devices with emitter size  $3 \times 10 \mu m^2$

We also compared the current gain and breakdown voltage  $BV_{CEO}$  in both devices with emitter size  $3 \times 10 \mu m^2$  and  $5 \times 10 \mu m^2$ . The increase in  $BV_{CEO}$  of  $3 \times 10 \mu m^2$  device is related to a smaller impact ionization due to the smaller current gain.

### RF performance for devices with emitter size $3 \times 10 \mu m^2$

The DC and RF performance for emitter size  $3 \times 10 \mu m^2$  is shown in Table 3. The transit time increases as the depleted collector thickness increases. The  $f_t$  is therefore decreases in power structures compared with high speed structures. Fig. 4 shows the  $f_t-I_c$  and  $f_{max}-I_c$  curves with  $V_{cb}=0.5V, 1.0V$  and  $3.0V$  for sample C. The emitter size is  $3 \times 10 \mu m^2$ . The peak  $f_t$  and  $f_{max}$  are around 40GHz and 140GHz at  $I_c=14mA$ , respectively. A comparison of  $f_t$  versus  $BV_{ceo}$  shows a strong relation to the collector thickness. We previous reported  $BV_{ceo}=11V$  and  $f_t=69GHz$  with collector thickness 500nm, and  $BV_{ceo}=6V$  and  $f_t=93GHz$  with collector thickness 250nm[2].

### Conclusions

We designed and processed 3 power InGaP HBT structures. Though the surface recombination current decreases the current gain of smaller devices  $3 \times 10 \mu m^2$ , the DC and RF performance meet the requirements for 2.4GHz circuit applications for sample C.

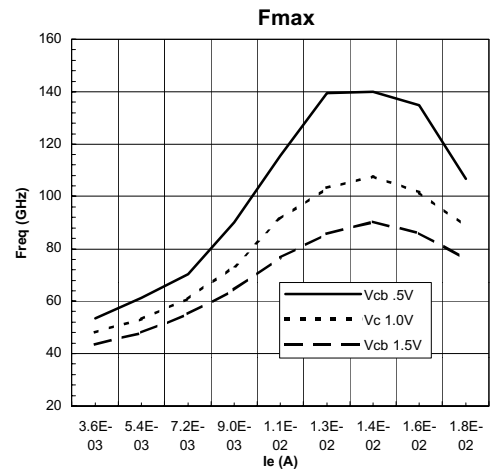
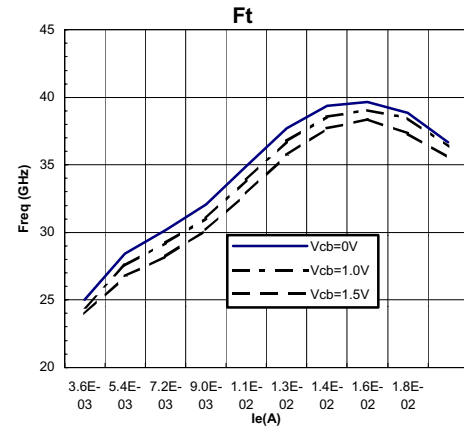


Fig. 4  $f_t$  and  $f_{max}$  of sample with a emitter size  $3 \times 10 \mu m^2$

## References

- [1] William Liu, "Handbook of III-V heterojunction bipolar transistors", John Wiley & Sons, Inc. pp. 299-301
- [2] D. A. Ahmari, Q.J. Hartmann, P.D. Meyer, M.L. Hattendorf, Q. Yang, J. Mu, M. Feng, and G. E. Stillman, "InGaP/GaAs HBTs with  $f_t$  and  $f_{max} > 100\text{GHz}$ ", GaAs ManTech Technical Digest, pp. 105-108
- [3] D. A. Ahmari, M. T. Fresina, Q. J. Hartmann, D. W. Barlage, P. J. Mares, M. Feng, G. E. Stillman, "High-speed InGaP/GaAs HBT's with a strained  $\text{In}_x\text{Ga}_{1-x}\text{As}$  Base," *IEEE Electron. Dev. Lett.*, vol. 17, pp. 226-228, 1996